Author(s): Leino, Teppo; Noutsias, Dimitris; Helttunen, Kaisa; Moilanen, Jani; Tarkkonen, Eeki; Kalenius, Elina; Kiesilä, Anniina; Pihko, Petri M.

Title: Hypersensitive Inhibition of Organocatalysts by Halide Salts : Are Two Catalysts Involved in the Mannich Reaction?

Year: 2024

Version: Published version

EurJOC
European Journal of Organic Chemistry

Research Article
doi.org/10.1002/ejoc.202400321

Chemistry Europe
European Chemical Societies Publishing

www.eurjoc.org

Hypersensitive Inhibition of Organocatalysts by Halide Salts: Are Two Catalysts Involved in the Mannich Reaction?

Teppo O. Leino,[a] Dimitris Noutsias,[a] Kaisa Helttunen,[a] Jani O. Moilanen,[a] Eeki Tarkkonen,[a] Elina Kalenius,[a] Anniina Kiesilä,[a] and Petri M. Pihko*[a]

Conformationally flexible tertiary amine – thiourea–urea catalysts **1** and **2** for the Mannich reaction between imines and malonate esters are efficiently inhibited by quaternary ammonium halides. NMR titrations, isothermal titration calorimetry (ITC) and NOE experiments showed that the catalysts bind chloride and bromide ions with relatively high affinities ($K = 10^3$–10^5 M^{-1} in acetonitrile). The halide ions not only block the active site of the catalysts, but they also induce refolding into catalytically inactive conformations upon complexation in an allosteric-like event. At substoichiometric inhibitor:catalyst ratios, the catalysts displayed hypersensitivity to the inhibitors, with overall rates that were lower than those expected from simple 1st order kinetics and 1 : 1 inhibitor:catalyst stoichiometry. To rationalize the observed hypersensitivity, different kinetic scenarios were examined. For catalyst **2** and the Takemoto catalyst (**6**), the data is consistent with 2nd order dependency on catalyst concentration, suggesting that a mechanism involving only a single catalyst in the catalytic cycle is not operative. For catalyst **1**, an alternative scenario involving 1st order in catalyst and catalyst poisoning at low concentrations of **1** could also rationalize the hypersensitivity. Interestingly, inhibition of catalysts **1** and **2** by halide salts led to significant loss of enantioselectivity, in contrast to the Takemoto catalyst **6** which was inhibited but with essentially no change in enantioselectivity.

Introduction

Halide ions are commonly encountered as modulators in proteins. In particular, chlorides play an important role in activation and deactivation of several enzyme families.[1] Examples of enzymes with characterized chloride binding sites include α-amylases (Figure 1),[2] angiotensin-converting enzyme I,[3] and WNK kinase 4.[4] In chloride-dependent amylases, the binding of chloride is believed to alter the acid/base properties of the key aspartate/glutamate residues at the active site.

In principle, synthetic catalysts could be similarly modulated by anion binding. Anion-mediated allosteric or allosteric-like[5] control of catalytic performance could enable tuning of the activity and selectivity of the small-molecule catalyst without the need to synthesize a new catalyst each time for a new application. In order to be able to elicit such a response, the synthetic catalysts should not only display high affinities for the regulatory anions, but they should also change their conformation upon binding to the anion[6] so that the catalytic site is affected as well. Changes of conformation upon anion binding have been demonstrated for pseudorotaxanes,[7] [3]rotaxanes,[8] foldamers[9] and fluorescent sensors[10]. Switchable catalysts that respond to light, pH and metal coordination are also known.[11] However, anion controlled switching and conformational response of supramolecular catalysts is extremely rare,[12] and to the best to our knowledge, our system represents the first example of a metal-free organocatalyst displaying a change in the folding pattern and catalytic response upon anion binding.

Herein we report the inhibition of small-molecule urea–thiourea catalysts **1** and **2** (Figure 1)[13–15] by Cl^- and Br^- salts in organic solvents. The halides refold the catalyst to an inactive conformation, disrupting the active site cleft of the catalyst.[16]

Results and Discussion

Catalysts **1** and **2** catalyze the Mannich reaction between imines and malonate esters or β-keto esters (Scheme 1).[13–15] **1** and **2** readily switch between different conformational states depending on the anion.[16] In the presence of organic acids, such as trifluoroacetic acid or hexafluoroacetylacetone (hfacac), the catalysts exhibit an intramolecularly hydrogen bonded folded structure characterized by an active site cleft (native fold). In contrast, with halide ions, the catalysts refold to accommodate the halide ion inside of the catalyst (anion receptor fold). Computational studies[13,14] suggest that these catalysts prefer the native fold also with actual substrates, dimethyl malonate (**4**, Scheme 1) and imines (e.g. **3**) since this fold can readily accommodate both substrates.

We hypothesized that halide ions should be particularly efficient inhibitors for these catalysts. The structures of the halide complexes in both solution and the solid state[16] do not

[a] T. O. Leino, D. Noutsias, K. Helttunen, J. O. Moilanen, E. Tarkkonen, E. Kalenius, A. Kiesilä, P. M. Pihko
Department of Chemistry and NanoScience Center, University of Jyväskylä, FI-40014 Jyväskylä, Finland
E-mail: petri.pihko@jyu.fi

Supporting information for this article is available on the WWW under https://doi.org/10.1002/ejoc.202400321

Research Article
doi.org/10.1002/ejoc.202400321

Chemistry Europe
European Chemical Societies Publishing

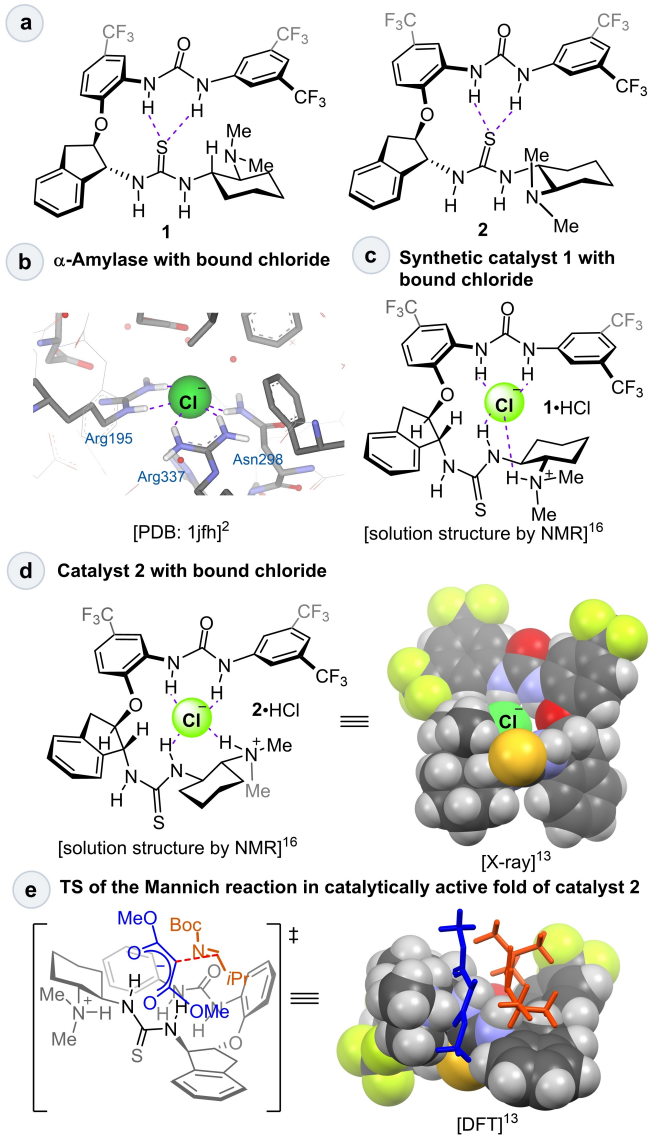

Figure 1. a) Structures of catalysts **1** and **2**. b) Example of an allosteric chloride-activated enzyme, α-amylase, with bound chloride ion near the active site. c) Structures of **1H$^+$Cl$^-$** and d) **2H$^+$Cl$^-$** (CCDC: YEKPIP) showing the catalytically inactive anion binding folds of the catalysts. e) Structure of the transition state (TS) for the Mannich reaction, showing the catalytically active native fold of **2**.

appear to possess suitable binding sites for the substrates. Thus, we hypothesized that halide ions could trap the active catalyst (Scheme 1), resulting in a catalytically inactive complex. The inhibition could theoretically take place either from the free catalyst (binding of chloride to the neutral catalyst) or by ion exchange with the binary complex intermediate (Scheme 1a).

We have previously established that hfacac complexes of catalysts **1** and **2** display an essentially complete shift to the conformationally refolded chloride complex **cat**H$^+$Cl$^-$ when titrated with a Cl$^-$ source *n*-Bu$_4$NCl (TBACl) (Scheme 1 b).[16] To obtain a more accurate value for K_{eq} for chloride complexation with the salt form of the catalyst, we used ITC titration with catalyst **2**H$^+$·hfacac$^-$. This experiment afforded $K_{eq} = (5.7 \pm 0.1) \cdot 10^5$ and $\Delta G = -32.9 \pm 0.12$ kJ mol^{-1} for the exchange reaction. For the corresponding bromide complex, a K_{eq} of $5.7 \cdot 10^3$ was obtained from NMR titration with *n*-Bu$_4$NBr. The hfacac salt was selected to mimic the dimethyl malonate substrate since the binary complex with malonate has a very low concentration[14] and cannot be observed by NMR. These trends were also reproduced by computational analysis. To reduce computational cost, Me$_4$N$^+$ cation was used instead of *n*-Bu$_4$N$^+$. The calculated value of ΔG for the reaction corresponding to Scheme 1b was −40.9 kJ·mol^{-1} at the M06-2X/def2-TZVPP level of theory (Table S37 in the Supporting Information (SI)), in good agreement with the experiments.[17]

However, due to low concentration of the **cat**H$^+$**mal**$^-$ binary complex under realistic reaction conditions,[18] trapping of the free catalyst with chloride ions is also possible (alternative A, Scheme 1 a). To explore this scenario, the binding constants of catalysts **1** and **2** with TBACl by NMR in CD$_3$CN were determined (SI, Section 3.1). The relatively high binding constants (**1**: $6.4 \cdot 10^3$ M^{-1} **2**: $2.1 \cdot 10^3$ M^{-1}) suggest that the neutral catalysts **1** and **2** could also be inhibited by chloride ions. Importantly, chloride binding resulted in refolding of the catalysts as evidenced by NOEs (Figure 2, see also Figs S52 and S56 of SI). Additional evidence for the formation of [**cat**·Cl]$^-$ species was provided by ESI-MS experiments, which showed abundant ion for [**cat**·Cl]$^-$ with both foldamers **1** and **2**. For both **1** and **2**, [**cat**Cl]$^-$ could be detected at *m/z* 782 (SI, Figs. S64–S65 and Table S38).

The results of the inhibition experiments are summarized in Table 1. Control experiments with potential halide salts indicated that TBACl exhibited sufficient solubility as well as low

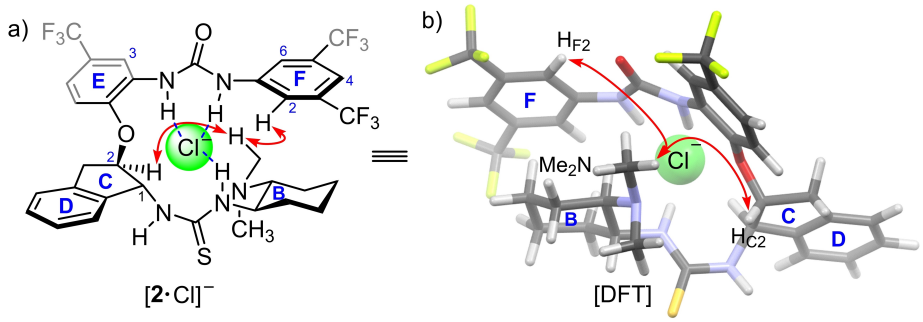

Figure 2. a) Solution structure of **TBA**$^+$ [**2**·Cl]$^-$ in CD$_3$CN and b) the computationally derived structure, with key NOESY correlations indicated by red arrows in both structures.

Research Article
doi.org/10.1002/ejoc.202400321

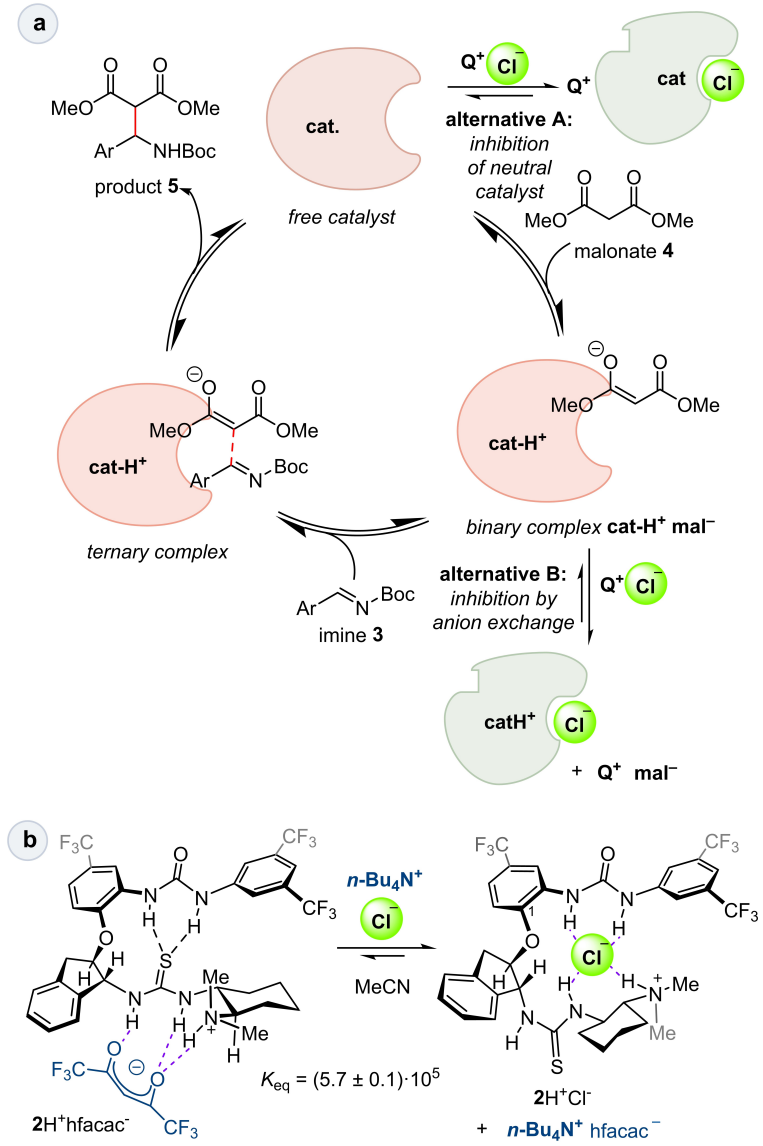

Scheme 1. a) Proposed simplified inhibition mechanism and b) equilibrium constant of the replacement of hfacac anion with the chloride anion in the salt $2H^+hfacac^-$.

catalytic activity on its own to be used as an inhibitor (SI, Fig. S6). C_6D_6 was selected as a solvent due to lower rate of background reaction compared to CD_3CN.[19] The inhibition experiments showed that under standard conditions ([**3**] = [**4**] = 0.23 M, C_6D_6) TBACl was clearly acting as an inhibitor for the Mannich reaction: with increasing [Cl^-], both the overall rates as well as the observed er's were uniformly decreased.[20] With an excess of TBACl (18 mol%, Table 1, entry 9), the catalyst was essentially inactive: no enantioselectivity was observed, and the reaction rate had dropped by a factor of 13. Both catalysts **1** and **2** were inhibited by TBACl and by TBABr (see entries 10 and 17). Variation of the [**3a**]:[**4**] ratio (see Table S7 in the SI) had essentially no effect on the inhibition. Furthermore, inhibition by TBACl was observed with both electron-rich imine **3b** and electron-poor imine **3c** (Table 2) without any noticeable difference in the inhibitory efficiency.

Interestingly, at substoichiometric inhibitor/catalyst ratios ([Cl^-]/[catalyst] < 1), the catalyst appeared to be hypersensitive to the inhibitor (Table 1, entries 4–6 and 14–15). For example, at 3 mol% (6.9 mM) TBACl and 22.9 mM of **1** or **2**, and 1:1 cat:Cl^- stoichiometry, at least 16 mM [**cat**] (70% of the original) should have remained, but the initial rate had fallen to 58 ± 9% or 48 ± 3% of the original rate (Table 1, entries 4 and 14).

This effect could be better quantified by estimating the effective concentration of the active catalyst ($[\mathbf{cat}]_{eff}$) from the reaction progress experiments using the Variable Time Normalization Analysis (VTNA) method of Bures.[21,22] We initially used a simple model where the reaction is first order in catalyst (SI, Figs. S25 and S28). At 6 mol% (13.6 mM) of inhibitor and 22.6 mM of catalyst, the theoretical concentration of the catalyst should be at least 9.0 mM, but VTNA (under the first order assumption) gives $[\mathbf{1}]_{eff\_VTNA1} = 6.0$ mM and $[\mathbf{2}]_{eff\_VTNA1} =$

Research Article
doi.org/10.1002/ejoc.202400321

Table 1. Inhibition experiments with catalysts **1** and **2** and TBAX salts (X=Cl or Br).

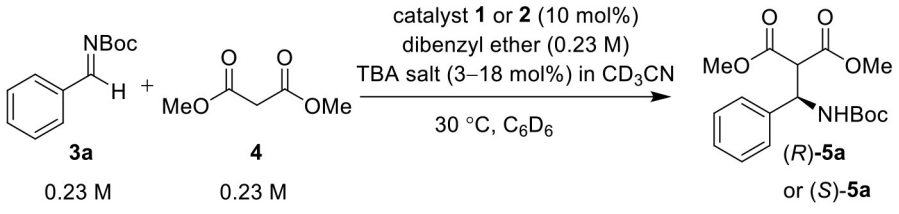

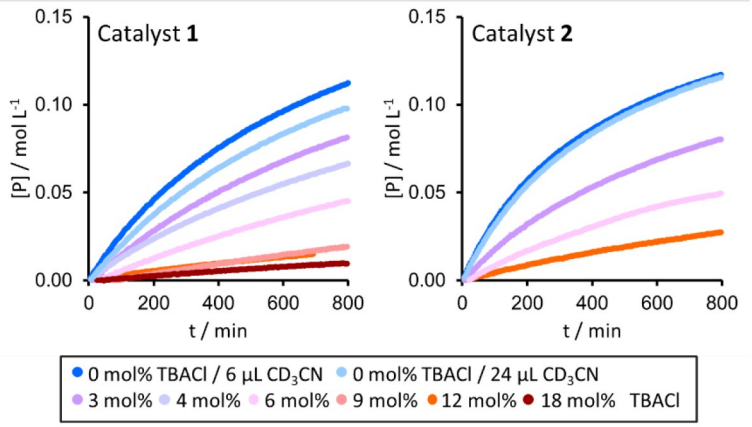

Entry	Cat.	X/TBAX (mol%)	Initial rate (mM min^{-1})	k/k_i[20]	*er* (*R*:*S*)
1	**1**	–/– [a]	0.35 ± 0.014	–	86:14
2	**1**	–/– [b]	0.21 ± 0.016	–	82:18
3	**1**	–/– [c]	0.16 ± 0.014	–	84:16
4	**1**	Cl/3	0.12 ± 0.015	1.7 ± 0.25	75:25
5	**1**	Cl/4	0.11	2.0	75:25
6	**1**	Cl/6	0.054 ± 0.0073	3.8 ± 0.59	73:27
7	**1**	Cl/9	0.023 ± 0.0011	6.2 ± 0.54	57:43
8	**1**	Cl/12	0.017 ± 0.0025	9.3 ± 1.6	61:39
9	**1**	Cl/18	0.012 ± 0.0005	12.9 ± 1.3	51:49
10	**1**	Br/12	0.037	4.3	73:27
11	**2**	–/– [a]	0.46 ± 0.048	–	6:94
12	**2**	–/– [b]	0.35 ± 0.011	–	3:97
13	**2**	–/– [c]	0.32 ± 0.0018	–	14:86
14	**2**	Cl/3	0.17 ± 0.0082	2.0 ± 0.11	3:97
15	**2**	Cl/6	0.069 ± 0.0054	5.0 ± 0.46	16:84
16	**2**	Cl/12	0.033 ± 0.0007	9.6 ± 0.21	36:64
17	**2**	Br/12	0.056	5.6	25:75

[a] Without added CD_3CN. [b] With 6 µL CD_3CN. [c] With 24 µL CD_3CN.

4.1 mM. Similarly, at 3 mol% (6.9 mM) of inhibitor, the theoretical $[\mathbf{cat}]_{eff\_theor} = 16.0$ mM, but VTNA gives $[\mathbf{1}]_{eff\_VTNA1} = 13.1$ mM and $[\mathbf{2}]_{eff\_VTNA1} = 9.8$ mM.

To rationalize the observed hypersensitivity, three different hypotheses were experimentally explored. The first hypothesis involves a catalytic cycle where the formation of the **catH$^+$mal$^-$** binary complex is the turnover-determining step. In this case, even substoichiometric [TBACl] would be sufficient to lower [**catH$^+$mal$^-$**] significantly and hence affect the overall rate since the formation of the binary complex would be slow. To examine this possibility, we carried out the reaction with 2,2-dideuterated malonate ester **4**-d_2, **3a**, and catalyst **1**. These experiments afforded a kinetic isotope effect (KIE) k_H/k_D of 1.33 ± 0.13 (without inhibitor) and k_H/k_D of 1.57 ± 0.25 (with 12 mol% TBACl) (SI, section 2.11). The relatively low 1° KIE is inconsistent with a turnover-determining deprotonation of **4**, suggesting that the first scenario is not operative. Further control experiments with varying [**3a**] and [**4**] established that both

Table 2. Inhibition experiments with catalyst **1** and imines **3b** and **3c**.

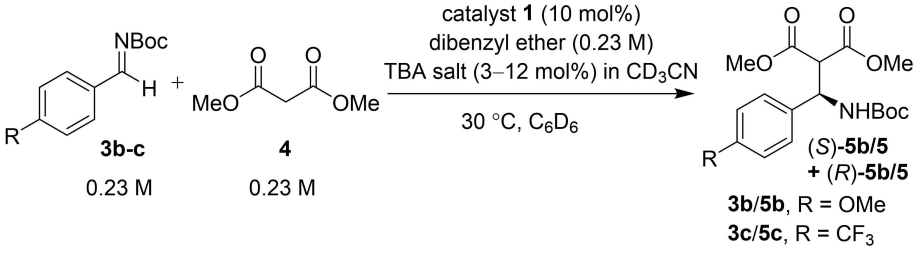

Entry	Catalyst/Imine	Inhibitor TBAX/amount (mol%)	Initial rate ($mM\,min^{-1}$)	k/k_i	*er (R:S)*
1	**1**/**3b**	–/–	0.042 ± 0.0049	–	86:14
2	**1**/**3b**	Cl/3	0.017 ± 0.0014	2.5 ± 0.36	75:25
3	**1**/**3b**	Cl/6	0.0069 ± 0.0009	6.2 ± 1.1	64:36
4	**1**/**3b**	Cl/12	0.0026 ± 0.0002	16.5 ± 2.2	61:39
5	**1**/**3c**	–/–	2.1	–	n.d.
6	**1**/**3c**	Cl/12	0.22	9.7	n.d.

substrates exhibit clear Michaelis-Menten saturation kinetics (for **3a**, $K_M = 0.68 \pm 0.13$ M and for **4**, $K_M = 0.54 \pm 0.05$ M, see SI, Section 2.2), and these experiments also confirmed that at low substrate concentrations, the reactions are approximately 1st order in both [**3a**] and [**4**]. These results agree with our earlier conclusion that C–C bond formation is likely the turnover-determining step in these Mannich reactions.[14]

A second hypothesis to rationalize the hypersensitivity involves the formation of 2:1 catalyst:inhibitor complexes. However, NMR titration experiments at 1.5 mM catalyst concentrations did not indicate formation of higher order complexes, although $[\mathbf{1}H\cdot\mathbf{1}HCl]^+$ and $[\mathbf{2}H\cdot\mathbf{2}HCl]^+$ could be characterized by ESI-MS (SI, Figures S63 and S64).

Finally, the third hypothesis involves questioning the assumption that the reaction is first order in catalyst. The order in catalyst was initially examined by the VTNA protocol by carrying out experiments with catalysts **1** and **2** at different concentrations (Figure 3a). This analysis revealed that the Mannich reaction catalyzed by **1** or **2** appeared to be 2nd order in catalyst. Interestingly, VTNA analysis also indicated that the 2nd order dependency was also exhibited by the Takemoto catalyst (**6**) for the same reaction (see the SI, Figure S19).

Control experiments with added product and catalyst decay experiments starting at lower concentrations of the reactants (SI, Figures S22 and S23) indicated that neither product inhibition nor catalyst decay could explain the apparent 2nd order relationship. Varying the concentration of MeCN-d_3, the additive/co-solvent used in inhibition experiments, also had no effect on the rate (see the SI, Figure S35). We also plotted the initial rates vs. [catalyst] at constant substrate concentrations (0.23 M, Figure 3b), which confirmed the 2nd order dependency for catalyst **2**. However, during these experiments, we found that catalyst **1** turned out to exhibit solubility problems at >45 mM concentrations, especially without MeCN-d_3, and the rates were found to be erratic in single independent experiments. Furthermore, these experiments could not clearly rule out a scenario where the reaction is 1st order in catalyst but also irreversibly inhibited by a catalyst poison. In the presence of catalyst poison (exogenous inhibitor), the rate vs. [catalyst] plot would give zero or low rates at low [catalyst] but 1st order at higher [catalyst], providing a catalyst-rate plot that intercepts the x-axis at nonzero catalyst concentration. Indeed, this scenario also fits the data obtained for **6** (Figure 3b, centre).

To obtain more reliable data at low [catalyst], and to resolve this issue, we carried out experiments with sequential addition of catalyst from stock solution of catalyst to the reaction mixture (Figure 3c). The advantage of the sequential addition of catalyst is that these experiments represent essentially a single reaction batch, removing the variability between different experiments carried out at different times and possible impurities from different batches of **3a**. Since the addition of catalyst to the reaction mixture increases the volume of the solution, and at the same time the substrates are being consumed, the rates between different additions can only be compared by taking into account the changes in substrate concentrations. Fortunately, initial [**3a**] and [**4**] after each addition can be directly obtained from the NMR data. Figure 3c presents the relative rates adjusted for the variation in [**3a**] and [**4**] (i.e. rate/[**3a**][**4**]) for varying [**2**], [**6**] and [**1**], assuming 1st order in the substrates on the basis of saturation kinetics experiments, see above). In these experiments, the plot for catalyst **2** agrees with the data obtained by previous methods (VTNA and independent experiments, Figure 3a and 3b), showing a 2nd order dependency, and for the Takemoto catalyst (**6**), a 2nd order plot also fits the data. However, for catalyst **1**, the plot exhibited a linear slope (1st order), with an intercept at 3.4 mM [**1**]. This result suggests that catalyst poisoning by an exogenous inhibitor (catalyst poison) is a possibility, at least with catalyst **1**.

Research Article
doi.org/10.1002/ejoc.202400321

Chemistry Europe
European Chemical Societies Publishing

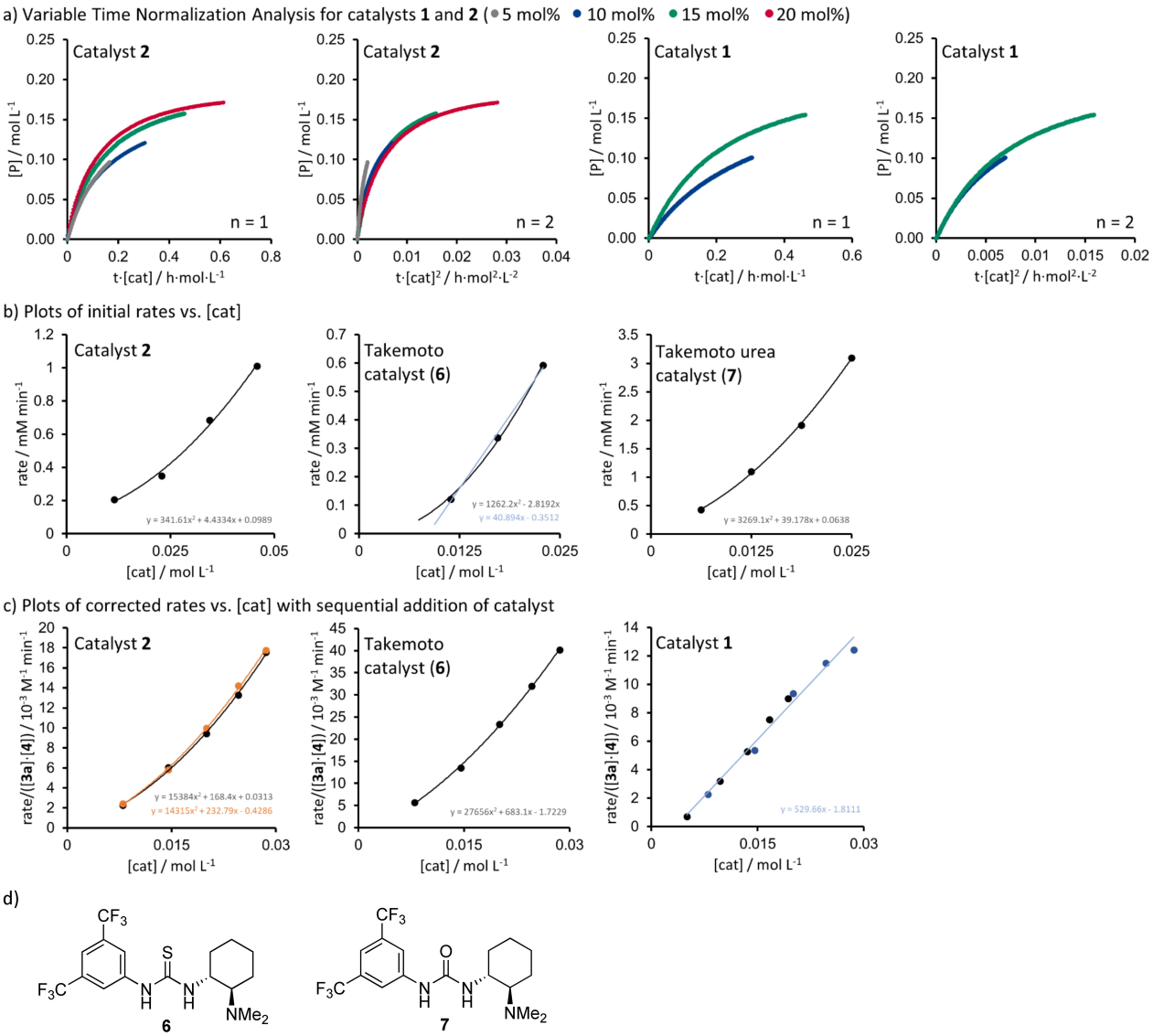

Figure 3. a) Variable Time Normalization Analysis for catalysts **1** and **2** at different catalyst concentrations: 1st order plots of [**5a**] = [**P**] vs. $\Delta t \cdot$[**cat**] (left) and 2nd order plots [**5a**] = [P] vs. $\Delta t \cdot$[**cat**]^2 (right). b) Plots of initial rates vs. [**cat**]. Each data point is derived from an independent kinetic measurement and the second-order fitting was used to connect them. In the case of Takemoto catalyst (**6**) also the linear fitting is presented (blue line). c) Plots of corrected initial rates vs. [**cat**] with sequential addition of catalyst. In the case of catalyst **2**, experiments with CD_3CN (black) and without CD_3CN (orange) are presented in the same graph. Black and blue data points in the graph of catalyst **1** are derived from two separate experiments. d) Structures of Takemoto catalyst (**6**) and Takemoto urea catalyst (**7**).

We would urge caution in interpreting these results for catalyst **1**. The solubility problems encountered with **1**, and literature precedents showing significant catalyst aggregation for thiourea catalysts[23,24] may partially mask the 2nd order relationship either via aggregation or undetected precipitation of the catalyst. Indeed, in all plots of Figure 3b and 3c, the plots appear linear or even curve downwards (catalyst **1**, Figure 3c) above ca. $25 \cdot 10^{-3}$ M catalyst. The entire purpose of these experiments was to provide a model for obtaining effective catalyst concentrations in the presence of the inhibitor TBACl at low [catalyst]. We remain agnostic whether the true order in catalyst is indeed different between catalyst **1** and the other catalysts studied herein, or whether **1** behaves differently due to solubility/aggregation effects.

To estimate the effective catalyst concentrations $[\mathbf{cat}]_{eff\_VTNA}$, we generated the VTNA plots with and without inhibitor (Figure 4) using the 1st order model with catalyst poisoning for catalyst **1** (Figures S25 and S26), and 2nd order model for both catalysts **1** and **2**. In the catalyst poison model for catalyst **1**, the theoretical catalyst concentrations $[\mathbf{1}]_{eff\_theor}$ were calculated by subtracting both the estimated concentration of the catalyst poison (3.4 mM) and $[TBACl]_0$ from $[\mathbf{1}]_0$ (assuming 1:1 binding of Cl^- to catalyst). $[\mathbf{2}]_{eff\_theor}$ was obtained by subtracting $[TBACl]_0$ from $[\mathbf{2}]_0$. An estimate for $[\mathbf{cat}]_{eff\_VTNA}$ was obtained by varying the $[\mathbf{cat}]_{eff}$ until the plots could be overlaid (see the Supporting Information, section 2.9). Importantly, under the assumption of 2nd order relationship for catalyst **2**, the estimated effective catalyst concentrations $[\mathbf{2}]_{eff\_VTNA2}$ (Figure 4) are either very close

Research Article
doi.org/10.1002/ejoc.202400321

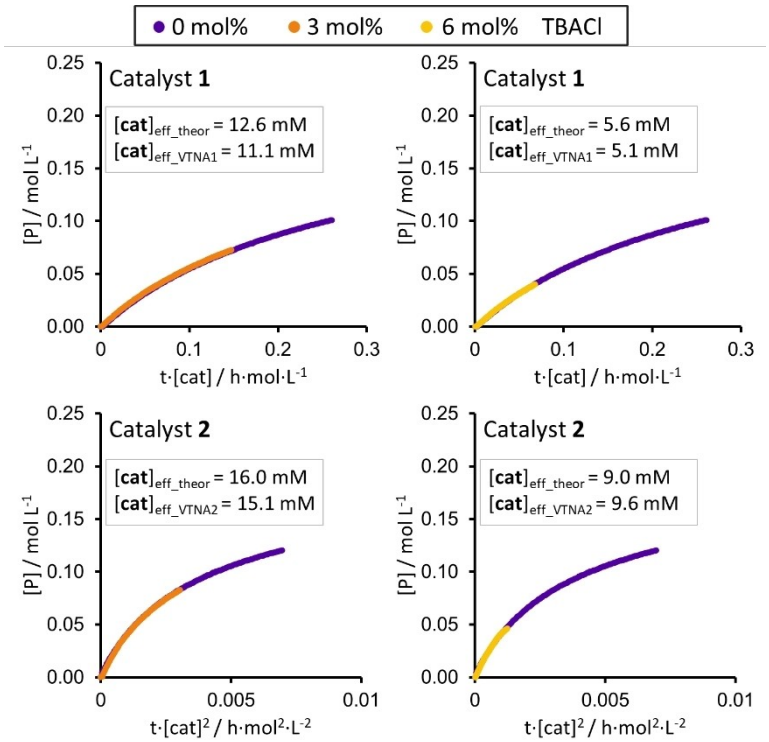

Figure 4. VTNA plots of [**P**] (**5**) with 22.6 mM (first curves) or 22.9 mM (second curves) catalysts **1** and **2** and 6.9 mM (orange) or 13.6 mM of inhibitor (yellow), overlaid with the plot without inhibitor (purple) under similar concentrations.

or even slightly below the theoretical catalyst concentrations $[\mathbf{cat}]_{eff\_theor}$, assuming 1:1 **cat**:$Cl^-$ stoichiometry and essentially complete inhibition. Similarly, for catalyst **1**, $[\mathbf{1}]_{eff\_VTNA1}$ obtained with the linear model are also very close to the theoretical values. The other models showed larger differences (see the SI, section 2.9).

Finally, we also examined whether the related Takemoto catalyst (**6**) displays similar sensitivity to chloride ion inhibition as **6** possesses fewer H-bond donor sites compared to **1** and **2**. As expected, catalyst **6** demonstrated significantly lower sensitivity to added chloride source. At 22 mM (10 mol%) of **6** and 26.4 mM (12 mol%) TBACl under the standard reaction conditions, significant catalytic activity remained, corresponding to ca. 6.6 mM $[\mathbf{cat}]_{eff\_VTNA2}$. The enantioselectivity also remained essentially unchanged (98:2 with no inhibitor vs. 97:3 er with 12 mol% TBACl; for details of experiments with **6**, see the SI, Sections 2.5 and 2.7).

Overall, the results show that the assumption of 1:1 catalyst:inhibitor stoichiometry appears to be valid, and this model can accurately predict effective catalyst concentrations for catalysts **1**, **2** and **6** without the need to invoke 2:1 complexes.

The apparent 2nd order dependency on **6** the Mannich reaction is surprising. In previous studies, the Michael reaction between the same nucleophile **3** and 2-nitrostyrene catalyzed by **6** has been determined to be 1st order in catalyst **6**.[25] The divergent kinetic behaviour with the same catalyst and same substrate but only with a different second substrate (imine **4**, 2nd order in **6** *vs.* 2-nitrostyrene, 1st order in **6**) is remarkable. To the best of our knowledge, such divergence in catalyst behaviour is unprecedented.

The combined evidence of the present work (i.e. saturation kinetics on [**3**] and [**4**] and 2nd order in catalyst) and our previous work[14] requires a revision of our previously proposed mechanism. Saturation kinetics provides clear evidence that **3** and **4** can reversibly bind to the catalyst. On-cycle catalyst dimerization, which has been proposed previously for thiourea catalysts,[26] may account for the apparent 2nd order in catalyst.[22] A revised mechanism, applicable to catalysts **2**, **6** and **7**, is presented in Scheme 2. In the proposed catalytic cycle, the productive merger of the initially formed binary catalyst-substrate complexes results in the formation of the quaternary complex, which proceeds to give the product in the turnover-determining, C–C bond forming event.

In enzymes, buried chloride coordination numbers typically range between 3 and 5.[27] However, in aqueous solution, chloride ions have a coordination number 6,[28] and synthetic urea/thiourea receptors typically form 4 to 6 hydrogen bonds to chloride.[29–33] In the 1:1 stoichiometry, $[catCl]^-$ is coordinated to only three H-bond donors. We believe that our catalysts **1** and **2**, although efficiently and stoichiometrically inhibited by chloride ions in this study, are still not ideal matches for Cl^-, leaving room for optimization. The strong binding of chloride ions observed herein could also be exploited in allosteric-like activation instead of inhibition, analogous to the known chloride-activated enzymes.

Research Article
doi.org/10.1002/ejoc.202400321

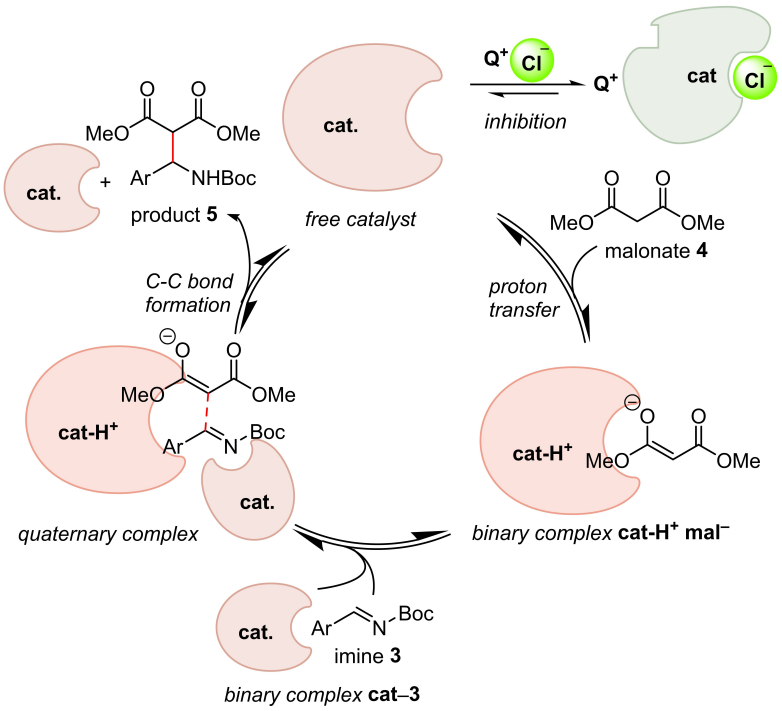

Scheme 2. Revised mechanism of the Mannich reaction catalysed by catalysts **2**, **6** and **7**, with two catalyst molecules involved in the turnover-determining C–C bond formation step.

Conclusions

In summary, we have demonstrated the capacity of conformationally flexible urea–thiourea catalysts **1** and **2** to be efficiently inhibited by tetra-*n*-butylammonium chloride. The chloride ions competitively bind to the catalysts with concomitant conformational change in the catalyst. The observed hypersensitivity of the catalysts to the inhibitors could be rationalized by a surprising 2nd order catalyst dependency of the Mannich reaction between **3** and **4**, or alternatively with a model involving a catalyst poison and 1st order in catalyst. Other hypotheses, such as slow deprotonation of **4**, higher order catalyst:inhibitor complexes, product inhibition or catalyst decay are not supported by the experiments. A revised mechanism involving two catalyst molecules is proposed. Studies to rationalize these results and utilization of the chloride-dependent switching in other organocatalysts are in progress.

Supporting Information

Additional references cited within the Supporting Information.[34–48] Experimental details, reaction progress plots, copies of representative NMR spectra and HPLC chromatograms (PDF).

Numerical Reaction Progress Data (XLSX)

XYZ coordinates of computed structures (ZIP).

Acknowledgements

We acknowledge financial support from the Department of Chemistry and the NanoScience Center, University of Jyväskylä (project FoBiCa), and support from the Research Council of Finland (projects 297874, 322899, 339892 (to P.M.P), 309910, 314287, 335685 and 339893 (to K.H.), 330800 (to T.O.L.), and 315829 and 338733 (to J. O. M.). The CSC-IT Centre for Science in Finland, the Finnish Grid and Cloud Infrastructure (persistent identifier urn:nbn:fi:research-infras-2016072533), and Prof. H. M. Tuononen (University of Jyväskylä) are acknowledged for providing computational resources. We also thank Mr. Esa Haapaniemi for assistance with NMR spectroscopy, and Dr. Imre Pápai and Dr. Ádám Madarász (TTK, Budapest, Hungary) for valuable discussions.

Conflict of Interests

The authors declare no conflict of interest.

Data Availability Statement

The data underlying this study are available in the published article and its Supporting Information.

Keywords: halides · Mannich reaction · inhibition · reaction mechanisms · conformational change

[1] R. K. Skitchenko, D. Usoltsev, M. Uspenskaya, A. V. Kajava, A. Guskov, *Bioinformatics* **2020**, *36*, 3064–3071.
[2] R. Maurus, A. Begum, H.-H. Kuo, A. Racaza, S. Numao, C. Andersen, J. W. Tams, J. Vind, C. M. Overall, S. G. Withers, G. D. Brayer, *Protein Sci.* **2005**, *14*, 743–755.
[3] C. A. Rushworth, J. L. Guy, A. J. Turner, *FEBS J.* **2008**, *275*, 6033–6042.
[4] J.-C. Chen, Y.-F. Lo, Y.-W. Lin, S.-H. Lin, C.-L. Huang, C.-J. Cheng, *Proc. Natl. Acad. Sci. USA* **2019**, *116*, 4502–4507.
[5] Allosteric effectors bind at a site other than the active site of the catalyst. In our case, the chloride ions bind to the urea subunit, disrupting the fold of the catalyst, and also to one of the thiourea N–Hs at the active site. Since the binding involves a conformational change resulting in the capture of an inactive conformation (i.e. it changes the populations of the conformers), it closely resembles true allosteric response and hence the term "allosteric-like" is used herein. For an example of allosteric capture of inactive conformation in enzymes, see: a) G. M. Lee, T. Shahian, A. Baharuddin, J. E. Gable, C. S. Craik, *J. Mol. Biol.* **2011**, *411*, 999–1016; For a discussion of conformer populations and allosteric effects, see: b) N. M. Goodey, S. J. Benkovic, *Nat. Chem. Biol.* **2008**, *4*, 474–482.
[6] P. A. Gale, E. N. W. Howe, X. Wu, *Chem.* **2016**, *1*, 351–422.
[7] G. T. Spence, C. Chan, F. Szemes, P. D. Beer, *Dalton Trans.* **2012**, *41*, 13474–13485.
[8] T. A. Barendt, I. Rašović, M. A. Lebedeva, G. A. Farrow, A. Auty, D. Chekulaev, I. V. Sazanovich, J. A. Weinstein, K. Porfyrakis, P. D. Beer, *J. Am. Chem. Soc.* **2018**, *140*, 1924–1936.
[9] Y. Hua, A. H. Flood, *J. Am. Chem. Soc.* **2010**, *132*, 12838–12840.
[10] Y. Bai, B.-G. Zhang, J. Xu, C.-Y. Duan, D.-B. Dang, D.-J. Liu, Q.-J. Meng, *New J. Chem.* **2005**, *29*, 777–779.
[11] V. Blanco, D. A. Leigh, V. Marcos, *Chem. Soc. Rev.* **2015**, *44*, 5341–5370.
[12] H. J. Yoon, J. Kuwabara, J.-H. Kim, C. A. Mirkin, *Science (1979)* **2010**, *330*, 66–69.
[13] N. Probst, Á. Madarász, A. Valkonen, I. Pápai, K. Rissanen, A. Neuvonen, P. M. Pihko, *Angew. Chem. Int. Ed.* **2012**, *51*, 8495–8499.
[14] A. J. Neuvonen, T. Földes, Á. Madarász, I. Pápai, P. M. Pihko, *ACS Catal.* **2017**, *7*, 3284–3294.
[15] A. J. Neuvonen, P. M. Pihko, *Org. Lett.* **2014**, *16*, 5152–5155.
[16] A. J. Neuvonen, D. Noutsias, F. Topić, K. Rissanen, T. Földes, I. Pápai, P. M. Pihko, *J. Org. Chem.* **2019**, *84*, 15009–15019.
[17] A slightly smaller negative value of ΔG ($-18\ kJ\cdot mol^{-1}$) was obtained at the PBE0/def2-TZVPP level. For further details, see the Supporting Information.
[18] In our previous studies with these catalyst scaffolds, we were unable to detect the malonate-catalyst complexes by NMR titration studies. See ref [14].
[19] 12 mol% TBACl gave a background rate of $0.0087 \pm 0.0045\ mM\,min^{-1}$ for the reaction between **3a** and **4** (both 0.22 M in C_6D_6) vs. $0.040\ mM\,min^{-1}$ in CD_3CN (see the Supporting Information for details).
[20] TBACl and TBABr were not sufficiently soluble in pure C_6D_6 to enable the preparation of a concentrated stock solution of the inhibitors in C_6D_6, and they were therefore added as solutions in CD_3CN. To correct for the inhibitory effect of added CD_3CN, rates obtained with 3–6 mol% of inhibitor are compared to the background rate with 6 μL of added CD_3CN and the rates with 9–18 mol% inhibitor are compared to the corresponding values with 24 μL of of added CD_3CN, corresponding approximately to the quantities of solvent added (SI, section 2.4.4). It should also be noted that the er's obtained at NMR probe temperatures are lower than those obtained under optimized conditions at 0 °C, see refs [13] and [14].
[21] J. Burés, *Angew. Chem. Int. Ed.* **2016**, *55*, 16084–16087.
[22] C. Alamillo-Ferrer, G. Hutchinson, J. Burés, *Nat. Chem. Rev.* **2023**, *7*, 26–34.
[23] G. Tárkányi, P. Király, T. Soós, S. Varga, *Chem. Eur. J.* **2012**, *18*, 1918–1922.
[24] D. D. Ford, D. Lehnherr, C. R. Kennedy, E. N. Jacobsen, *J. Am. Chem.* **2016**, *138*, 7860–7863.
[25] T. Okino, Y. Hoashi, T. Furukawa, X. Xu, Y. Takemoto, *J. Am. Chem.* **2005**, *127*, 119–125.
[26] Y. Fan, S. R. Kass, *J. Org. Chem.* **2017**, *82*, 13288–13296.
[27] O. Carugo, *BMC Struct. Biol.* **2014**, *14*, 19.
[28] A. Bankura, B. Santra, R. A. DiStasio, C. W. Swartz, M. L. Klein, X. Wu, *Mol. Phys.* **2015**, *113*, 2842–2854.
[29] P. Yang, J. Wang, C. Jia, X.-J. Yang, B. Wu, *Eur. J. Org. Chem.* **2013**, *2013*, 3446–3454.
[30] M. Olivari, R. Montis, S. N. Berry, L. E. Karagiannidis, S. J. Coles, P. N. Horton, L. K. Mapp, P. A. Gale, C. Caltagirone, *Dalton Trans.* **2016**, *45*, 11892–11897.
[31] X. Wu, L. W. Judd, E. N. W. Howe, A. M. Withecombe, V. Soto-Cerrato, H. Li, N. Busschaert, H. Valkenier, R. Pérez-Tomás, D. N. Sheppard, Y.-B. Jiang, A. P. Davis, P. A. Gale, *Chem.* **2016**, *1*, 127–146.
[32] N. Busschaert, M. Wenzel, M. E. Light, P. Iglesias-Hernández, R. Pérez-Tomás, P. A. Gale, *J. Am. Chem.* **2011**, *133*, 14136–14148.
[33] D. Meshcheryakov, F. Arnaud-Neu, V. Böhmer, M. Bolte, V. Hubscher-Bruder, E. Jobin, I. Thondorf, S. Werner, *Org. Biomol. Chem.* **2008**, *6*, 1004–1014.
[34] S. Handa, V. Gnanadesikan, S. Matsunaga, M. Shibasaki, *J. Am. Chem. Soc.* **2010**, *132*, 4925–4934.
[35] F. Perez, Y. Ren, T. Boddaert, J. Rodriguez, Y. Coquerel, *J. Org. Chem.* **2015**, *80*, 1092–1097.
[36] C. Frassineti, S. Ghelli, P. Gans, A. Sabatini, M. S. Moruzzi, A. Vacca, *Anal. Biochem.* **1995**, *231*, 374–382.
[37] M. Ernzerhof, G. E. Scuseria, *J. Chem. Phys.* **1999**, *110*, 5029–5036.
[38] C. Adamo, V. Barone, *J. Chem. Phys.* **1999**, *110*, 6158–6170.
[39] Y. Zhao, D. G. Truhlar, *Theor. Chem. Acc.* **2008**, *120*, 215–241.
[40] S. Grimme, S. Ehrlich, L. Goerigk, *J. Comput. Chem.* **2011**, *32*, 1456–1465.
[41] B. P. Pritchard, D. Altarawy, B. Didier, T. D. Gibson, T. L. Windus, *J. Chem. Inf. Model.* **2019**, *59*, 4814–4820.
[42] F. Weigend, R. Ahlrichs, *Phys. Chem. Chem. Phys.* **2005**, *7*, 3297–3305.
[43] M. J. Frisch, G. W. Trucks, H. B. Schlegel, G. E. Scuseria, M. A. Robb, J. R. Cheeseman, G. Scalmani, V. Barone, G. A. Petersson, H. Nakatsuji, X. Li, M. Caricato, A. V. Marenich, J. Bloino, B. G. Janesko, R. Gomperts, B. Mennucci, H. P. Hratchian, J. V. Ortiz, A. F. Izmaylov, J. L. Sonnenberg, D. Williams-Young, F. Ding, F. Lipparini, F. Egidi, J. Goings, B. Peng, A. Petrone, T. Henderson, D. Ranasinghe, V. G. Zakrzewski, J. Gao, N. Rega, G. Zheng, W. Liang, M. Hada, M. Ehara, K. Toyota, R. Fukuda, J. Hasegawa, M. Ishida, T. Nakajima, Y. Honda, O. Kitao, H. Nakai, T. Vreven, K. Throssell, J. A., Jr. Montgomery, J. E. Peralta, F. Ogliaro, M. J. Bearpark, J. J. Heyd, E. N. Brothers, K. N. Kudin, V. N. Staroverov, T. A. Keith, R. Kobayashi, J. Normand, K. Raghavachari, A. P. Rendell, J. C. Burant, S. S. Iyengar, J. Tomasi, M. Cossi, J. M. Millam, M. Klene, C. Adamo, R. Cammi, J. W. Ochterski, R. L. Martin, K. Morokuma, O. Farkas, J. B. Foresman, D. J. Fox, Gaussian 16, Revision C.01, Gaussian, Inc., Wallingford CT, **2016**.
[44] V. Gabelica, A. A. Shvartsburg, C. Afonso, P. Barran, J. L. P. Benesch, C. Bleiholder, M. T. Bowers, A. Bilbao, M. F. Bush, J. L. Campbell, I. D. G. Campuzano, T. Causon, B. H. Clowers, C. S. Creaser, E. De Pauw, J. Far, F. Fernandez-Lima, J. C. Fjeldsted, K. Giles, M. Groessl, C. J. Hogan Jr, S. Hann, H. I. Kim, R. T. Kurulugama, J. C. May, J. A. McLean, K. Pagel, K. Richardson, M. E. Ridgeway, F. Rosu, F. Sobott, K. Thalassinos, S. J. Valentine, T. Wyttenbach, *Mass Spectrom. Rev.* **2019**, *38*, 291–320.
[45] S. M. Stow, T. J. Causon, X. Zheng, R. T. Kurulugama, T. Mairinger, J. C. May, E. E. Rennie, E. S. Baker, R. D. Smith, J. A. McLean, S. Hann, J. C. Fjeldsted, *Anal. Chem.* **2017**, *89*, 9048–9055.
[46] E. Kalenius, M. Groessl, K. Rissanen, *Nat. Chem. Rev.* **2019**, *3*, 4–14.
[47] V. Gabelica, in *Ion Mobility-Mass Spectrometry: Fundamentals and Applications*, The Royal Society Of Chemistry, **2022**, pp. 1–25.
[48] V. Gabelica, E. Marklund, *Curr. Opin. Chem. Biol.* **2018**, *42*, 51–59.

Manuscript received: March 27, 2024
Revised manuscript received: April 4, 2024
Accepted manuscript online: April 8, 2024
Version of record online: May 7, 2024